

Multiphoton Spectroscopy of a Dynamical Axion Insulator

Olivia Liebman,^{*} Jonathan Curtis, Ioannis Petrides, and Prineha Narang[†]

College of Letters and Science, University of California, Los Angeles

(Dated: June 2, 2023)

The unusual magnetoelectric transport present in Weyl semimetals can be compactly understood as manifestations of an underlying axion field, which itself is determined by the microscopic band structure. The axion couples nonlinearly to electric and magnetic fields and possesses a signature topological magnetoelectric response, leading to a modified form of Maxwell's equations known as axion electrodynamics. Axions are naturally present in Weyl semimetals relating to the separation of the Weyl nodes in energy and in crystal momentum. In the presence of strong interactions, charge density-wave (CDW) order may develop which serves to gap the Weyl nodes and introduces corresponding collective excitations. When the inherent chiral symmetry of Weyl semimetals is spontaneously broken by the formation of CDW order, the resultant chiral condensate is endowed with intrinsic dynamics which yields a dynamical contribution to the axion field. However, unambiguous identification of this dynamical axion mode is challenging due to its inherent nonlinear coupling to electromagnetic fields. Therefore, we propose an all-optical protocol for verifying and characterizing dynamical axion collective modes in Weyl semimetals with CDW order. First, we show that axion collective mode can be excited using two-photon excitation schemes. Following excitation, the collective axion oscillations are then diagnosed by measuring the time-resolved Kerr rotation. Our results demonstrate a pathway towards utilizing multi-photon and entangled pair spectroscopies to identify new correlated phases in quantum matter.

Introduction—Axionic particles were originally proposed in high-energy physics in order to solve the charge-parity problem as the Nambu-Goldstone bosons associated with a new global axial U(1) symmetry [1, 2]. Today, axions are a leading dark matter candidate and could help explain the matter-antimatter asymmetry present in the universe [3]. While the axion has yet to be discovered in particle physics, its condensed matter [4] counterpart has been theorized to exist in certain three-dimensional materials [5–9]. A characteristic identifier of the presence of an axion is a signature magnetoelectric response, leading to a modified form of electrodynamics known as axion electrodynamics [10–12].

It turns out Weyl semimetals naturally have an axion term that is related to the separation in k-space and in energy of the Weyl nodes. What's more, when the Weyl system undergoes lattice translation symmetry breaking due to the emergence of charge density wave (CDW) order [13, 14], the collective motion associated to the phase of the CDW in turn leads to a dynamical axion effect and to a *nonlinear* magnetoelectric effect on top of the response due to band structure effects [15–18]. In the presence of uncompensated carrier densities this may even lead to spatially inhomogeneous textures due to softening of the axionic collective mode [19].

In addition to being of fundamental interest, there have also been proposals that the magnetoelectric coupling mediated by the axion response in materials may be of practical value, e.g., in nonreciprocal thermal emitters or rectifiers [20, 21]. However, while some progress has been made, techniques for the unambiguous identification of

dynamical axion quasiparticles are challenging, and often rely on studying linear perturbations in the presence of a strong magnetic field [5, 22–24].

Here we lay out an all-optical, contactless protocol for identification of nonlinear signatures of dynamical axions in a Weyl semimetal with CDW order. This protocol breaks down into two parts; first a dynamical axion mode is nonlinearly excited through two-photon processes, which carries a distinct dependence on the incident angle, polarization, and frequencies of the two beams. Following excitation, the induced axion dynamics are then detected through their manifestation in the Kerr angle rotation of a third reflected probe beam, which acts as a faithful proxy for the dynamical evolution of the axion in the material [25, 26]. More generally, our work demonstrates the potential of using entanglement pairs to identify correlated phases in quantum materials.

Axion electrodynamics—We now describe the excitation protocol, starting from a model for dynamical axion collective modes in a Weyl semimetal with CDW order. The simplest form to discuss Weyl physics is when time-reversal symmetry is broken but inversion symmetry is persevered, thus there are minimally two nodes of equal energy. The CDW Weyl Hamiltonian expanded near the degeneracy points is

$$\mathcal{H}(\mathbf{k}) = \begin{pmatrix} v_F \boldsymbol{\sigma} \cdot \mathbf{k} & \Delta \\ \Delta & -v_F \boldsymbol{\sigma} \cdot \mathbf{k} \end{pmatrix} \quad (1)$$

where v_F is the Fermi velocity, $\boldsymbol{\sigma}$ is the triplet of Pauli matrices, \mathbf{k} is the crystal momentum, and $\Delta = |\Delta|e^{i\theta}$ is the CDW term and is analogous to a complex mass term, also represented in terms of the gap amplitude $|\Delta|$ and phase θ . In an uncorrelated Weyl semimetal with no CDW $\Delta = 0$ the nodes are gapless. The chirality of the Weyl nodes is identical to the topological charge

^{*} oliebman@ucla.edu

[†] prineha@ucla.edu

associated to each band crossing, given by the Chern flux $C = +1/2$ ($C = -1/2$) for the right- (left-) handed Weyl particles [27]. This chiral charge can be understood as magnetic monopoles, or sources and sinks, of the Berry curvature which is singular at the nodes and acts as an effective magnetic field in reciprocal space [28].

In the presence of sufficiently strong interactions, a transition to CDW ordered phase with complex order parameter Δ can occur. If the order is incommensurate, by Goldstone's theorem this will have a soft sliding mode associated with the phase of the CDW order, $\theta(x)$. Due to the chiral anomaly, it is known that the phase of the complex CDW can be identified with the axion response [6] of the material. This serves to modify the electrodynamics of the medium, with Lagrangian

$$\mathcal{L}_{\text{EM}} = \frac{1}{2}(\epsilon \mathbf{E}^2 - \frac{1}{\mu} \mathbf{B}^2) + g\theta \mathbf{E} \cdot \mathbf{B}. \quad (2)$$

The first two terms are the sourceless Maxwell Lagrangian in terms of the electric (magnetic) fields \mathbf{E} (\mathbf{B}), and ϵ (μ) is the static dielectric (permeability) tensor (we use units with $\epsilon_0 = \mu_0 = 1$). The last term proportional to $\mathbf{E} \cdot \mathbf{B}$ is the so-called axion response that leads to a magnetoelectric coupling mediated by the CDW phase θ , with coupling constant $g = \alpha/\pi$.

The total CDW phase θ is given by

$$\theta(\mathbf{r}, t) = \mathbf{Q} \cdot \mathbf{r} + \delta\theta(\mathbf{r}, t), \quad (3)$$

where the first term is dubbed the static axion field as it depends only on the separation in momentum-space \mathbf{Q} between the Weyl nodes, and is determined by the band-structure of the material [29]. The second term $\delta\theta(\mathbf{r}, t)$ is the **dynamical axion field**, which can be understood as the collective mode associated to the sliding phase mode of the CDW.

The electromagnetic Lagrangian (2) is supplemented by the Nambu-Goldstone equations of motion of the collective dynamical axion mode, namely

$$\mathcal{L}_{\text{NG}} = \frac{\kappa}{2} [(\partial_t \delta\theta)^2 - v^2 (\nabla \delta\theta)^2 - \Omega_0^2 \delta\theta^2] \quad (4)$$

The first term in the above equation is the kinetic energy with κ the chiral compressibility, which is proportional to the density of states at the Fermi level; the second term describes the spatial dispersion with v the speed of sound in the medium; and the final term is the pinning-induced gap term with Ω_0 the pinning frequency.

The equations of motion of the gauge potential derived from Eq. (4) are given by

$$\partial_t^2 \mathbf{A} - \nabla \times \nabla \times \mathbf{A} = g(\partial_t \theta \nabla \times \mathbf{A} - \nabla \theta \times \partial_t \mathbf{A}) \quad (5)$$

where $\mathbf{B} = \nabla \times \mathbf{A}$ and $\mathbf{E} = \partial_t \mathbf{A}$ are the magnetic and electric fields, respectively, given in terms of the gauge potential with the Weyl gauge selected $\nabla \phi = 0$ for scalar potential ϕ . The current response of the axion insulator is hence

$$\mathbf{J} = g \nabla \theta \times \mathbf{E} + g \dot{\theta} \mathbf{B}. \quad (6)$$

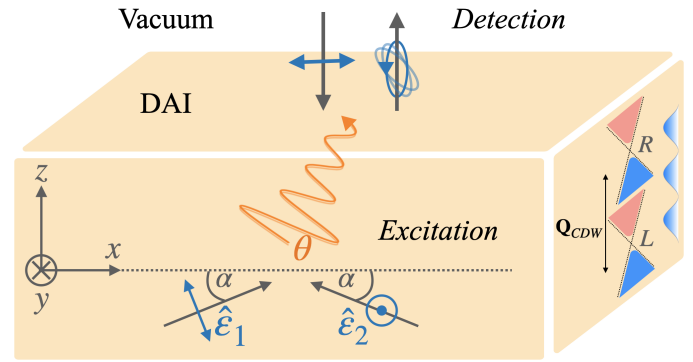


FIG. 1. Schematic of the general excitation and detection set-up. Two incident beams come in at a relative angle of $\pi - 2\alpha$ with polarizations $\hat{\epsilon}_1, \hat{\epsilon}_2$; frequencies ω_1, ω_2 ; and wave vectors $\mathbf{q}_1, \mathbf{q}_2$; and are used to induce finite $\mathbf{E} \cdot \mathbf{B}$, exciting an axionic collective mode using a multiphoton absorption event. In order to verify the creation of the axionic mode, time-resolved Kerr rotation can be used. For a probe beam at normal incidence (assumed to be collinear with the static axion response along \mathbf{Q}), the reflected beam's polarization will be elliptically polarized at an angle that oscillates in phase with the induced axion oscillations.

In particular, the first term is equivalent to an anomalous Hall response proportional to the spatial gradient of the axion field, while the second term is known as the chiral magnetic effect and is only relevant in the presence of time-dependent axion fields. The equations of motion for the dynamical axion $\delta\theta$ are

$$\kappa(\partial_t^2 + \gamma\partial_t - v^2\nabla^2 + \Omega_0^2)\delta\theta = g\mathbf{E} \cdot \mathbf{B} \quad (7)$$

Here the second term introduces a phenomenological damping parameter γ . These equations qualitatively describe massive sound waves driven by an effective force $g\mathbf{E} \cdot \mathbf{B}$. Thus as long as the electric and magnetic fields have some non-orthogonal component the collective dynamical axion field can be excited.

Exciting the dynamical axion mode—As seen in Eq. (7), exciting a dynamical axion mode in a material is a nonlinear optical process requiring at least two electromagnetic fields. In general, the intensity of the axion response depends on the frequency, momenta, polarization, and angle of the incident beams, see Fig. 1 for proposed protocol. We consider the following plane-wave ansatz $\mathbf{A}(q) = \mathbf{A}_1\delta_{q,q_1} + \mathbf{A}_2\delta_{q,q_2}$, where $q_i = (\omega_i, \mathbf{q}_i)$ is the four-momentum with ω_i the frequency and \mathbf{q}_i the momentum. The field amplitudes $\mathbf{A}_i = A_i\hat{\epsilon}_i$ are related to the polarizations $\hat{\epsilon}_i$ which obey $\mathbf{q}_i \cdot \hat{\epsilon}_i = 0$. We further assume that the momenta satisfy the free-space dispersion relations so that $|\mathbf{q}_i| = |\omega_i|$.

The response of the dynamical axion to the application of the vector potential $\mathbf{A}(q)$ is given by

$$\delta\theta(\omega_1, \omega_2, \mathbf{q}_1, \mathbf{q}_2) = \frac{(g/\kappa)(\omega_2\mathbf{q}_1 - \omega_1\mathbf{q}_2) \cdot (\hat{\epsilon}_1 \times \hat{\epsilon}_2)}{(\omega_1 + \omega_2)^2 + i(\omega_1 + \omega_2)\gamma - \Omega_0^2} A_1 A_2 \quad (8)$$

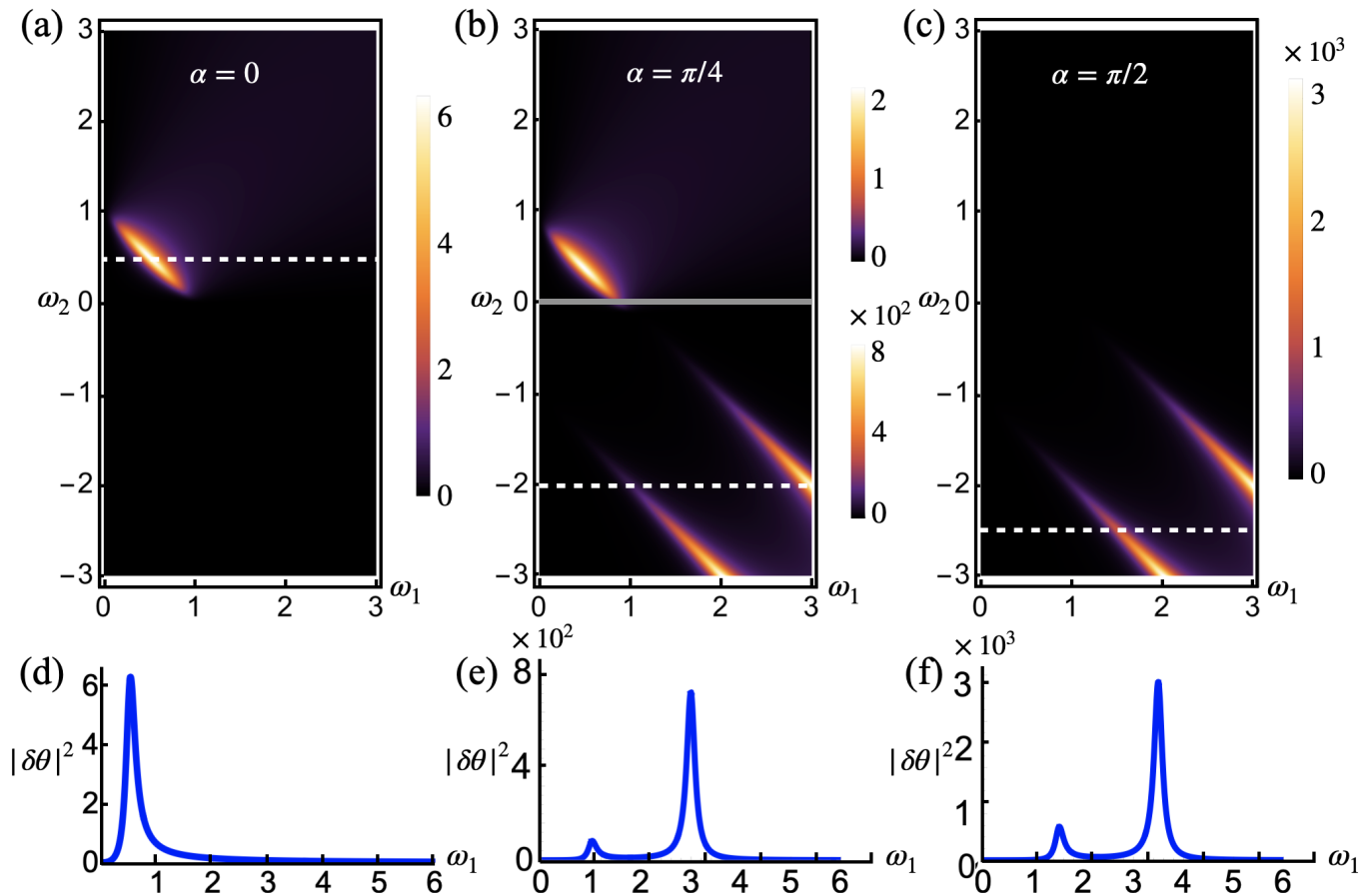


FIG. 2. Induced axion amplitude $|\delta\theta|^2$ as a function of incident photon frequencies ω_1, ω_2 for different incident angles α in the maximally-crossed polarization channel. (a) Excitation amplitude for $\alpha = 0$ (beams anti-parallel head on). We see a pronounced two-photon absorption feature when $\omega_2 + \omega_1 = \Omega_0$. (b) Orthogonal incidence when $\alpha = \pi/4$. We see that in addition to the two-photon absorption channel, we also see the emergence of a much stronger inelastic (stimulated Raman) excitation channel. Note the $y = 0$ line separates the two half planes, as well as note the separate scale bars for each. This was done to resolve the axion response in the upper half plane, which is significantly weaker as compared to the response shown in the lower half plane. (c) Parallel collinear incidence ($\alpha = \pi/2$). In this case, the two-photon absorption channel has been completely suppressed and instead the Raman excitation channel is maximal. Note in this case the relative momentum of the two beams is zero and therefore there must be a finite relative-frequency.

here the term proportional to $v^2 \nabla^2$ of Eq. (7) has been dropped since $v \ll c$. Importantly, the appearance of the vector triple product constrains the amplitude of the dynamical axion mode to the geometric volume defined by the two polarization vectors $\hat{\epsilon}_i$ and the relative four-momenta q_i of the incident electromagnetic fields; as a result, this provides a route towards smoking-gun identification of the axion collective mode.

In order to excite the axion, the polarizations must be non-collinear and also must be non-collinear with the relative four-momentum $\omega_1 \mathbf{q}_2 - \omega_2 \mathbf{q}_1$. In Fig. 2 we explore the efficacy of this two-photon excitation protocol for a variety of different incident beam angles α and frequencies ω_i in the maximally-crossed polarization channel, c.f., Fig. 1. Depending on the relative angle α there are two two-photon channels which can be used to excite the dynamical axion mode. Two-photon absorption can be used when the beams are close to head-on, i.e., $\alpha = 0$.

For parallel-propagating collinear beams, with $\alpha = \pi/2$ this channel is closed, and instead stimulated Raman excitation can be used to excite the dynamical axion mode by inelastic scattering of light. At intermediate incident angles, e.g., $\alpha = \pi/4$, both channels are active. Fig. 2 shows clearly how varying degrees of freedom of the incident beam will induce changes to axion excitation intensity, with the inelastic stimulated Raman channel for collinear beams resulting in a stronger response relative to the two-photon absorption process.

Axion detection via Kerr angle modulation—Now that the protocol for exciting an axion collective mode has been established, we move on demonstrate how it can be detected via an optical signature. The key idea is to use a linearly polarized detection beam of known frequency at normal incidence, to allow for optical detection of the axion field by its effect on the reflected light; a technique well established for the spectroscopy of static axion re-

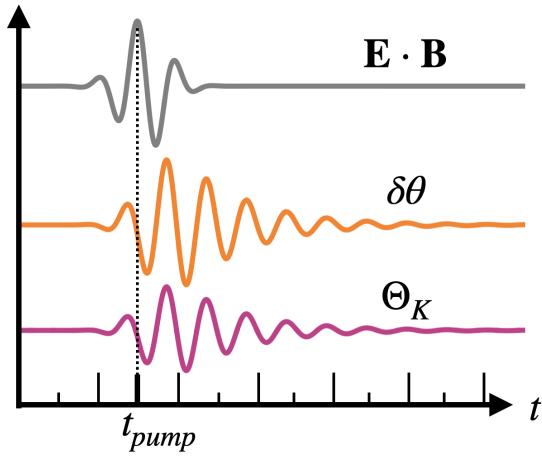


FIG. 3. Manifestations of excited axion collective mode in transient Kerr angle rotation. Using protocol established here the axion is pumped by a finite $\mathbf{E} \cdot \mathbf{B}$ profile, which is tuned to be in two-photon resonance with the dynamical axion. This induces collective oscillations of the axion angle shown above as $\delta\theta(t)$. These oscillations then manifest in the time-dependence of the Kerr-angle $\Theta_K(t)$ which approximately track the axion field. Parameters used here are: axion resonant frequency $\Omega_0 = 1$, axion damping $\gamma = 0.2$, constant $g = 0.1$, chiral compressibility $\kappa = 1$, probe frequency $\omega = 1$, and dielectric matrix elements $\epsilon_1 = 10$ and $\epsilon_2 = 0.7$. Note the amplitudes for each response are not to scale. The pump amplitude is an order of magnitude greater than the $\delta\theta$ amplitude, which is itself an order of magnitude greater than the Θ_K amplitude.

sponses [25].

The proposed pump-probe style protocol is illustrated in Fig. 1, where the pump beam excites the dynamical axion mode in the bulk and is bounded above by a vacuum with relative permittivity $\epsilon = 1$. For simplicity we assume the material is nonmagnetic so that $\mu = \mu_0 = 1$. Also, by assuming the probe incident beam wave vector along the z-axis, it is sufficient to consider the bulk dielectric permittivity tensor only in the plane orthogonal to the direction of propagation of the wave

$$\epsilon(\omega) = \begin{pmatrix} \epsilon_{xx} & \epsilon_{xy} \\ \epsilon_{yx} & \epsilon_{yy} \end{pmatrix} = \begin{pmatrix} \epsilon_1 & i\epsilon_2 \\ -i\epsilon_2 & \epsilon_1 \end{pmatrix} \quad (9)$$

where the dielectric tensor includes Hall effect contributions given as the complex off-diagonal matrix elements. Furthermore, we assume that the axion field's spatial variation is small compared to the wavelength of the incident light, such that $\nabla\delta\theta \ll q\delta\theta$ everywhere except close to the surface where we treat $\nabla\delta\theta$ as a sharp δ -function singularity. We also take the adiabatic approximation where $\partial_t\delta\theta \ll \omega\delta\theta$ such that contributions from the time derivative are sufficiently small so as to be taken to be zero, with the justification being that the axion frequency varies slowly as compared to the frequency of light. This will be later relaxed to allow for dynamical axion modes.

Under these assumptions Eq. (5) reduces to $\nabla \times \nabla \times \mathbf{A} = -\epsilon(\mathbf{r})\partial_t^2 \mathbf{A}$ in the medium. Solving for the

gauge potential \mathbf{A} naturally yields the chiral basis set $\mathbf{A}_j^\pm = A_j^\pm \frac{1}{\sqrt{2}}(1, \pm i)^T$ where A_j^\pm is an amplitude prefactor, and corresponding eigenvalues $q^\pm = \omega n^\pm$ with $n_\pm = \sqrt{\epsilon_1 \pm \epsilon_2}$. The reflectance and transmittance amplitudes can be obtained via the continuity of electric and magnetic fields at the interface, given as $\mathbf{E}_i + \mathbf{E}_r = \mathbf{E}_t$, and $\mathbf{B}_i + \mathbf{B}_r = \mathbf{B}_t + g\delta\theta \mathbf{E}_t$. We are most interested in nonlinear optics effects which may be detected using spectroscopic techniques. In turn, the coefficients of most use are the reflection coefficients, given in terms of the incident beam as

$$R^\pm = \pm \frac{1 \mp (n^\pm \mp ig\delta\theta)}{1 \pm (n^\pm \mp ig\delta\theta)} I^\pm \quad (10)$$

Here I^\pm denotes the incident light written in the chiral basis. The plus/minus reflection coefficients are, in general, different for left- and right-circularly polarized light.

To promote $\delta\theta$ to time-dependence, the partial differential equation of Eq. (7) are solved with the initial condition $\delta\theta(t \ll t_{pump}) = 0$ as the axion field is not excited before the onset of the pump at time t_{pump} . Following excitation, the damping term γ causes a ring down of the axion field, see Fig. 3. The key result is the reflection amplitude's direct dependence on the axion field. This will manifest as a modulation of the reflected beam Kerr angle, and serves as our smoking gun optical signature to unambiguously deduce the presence of a dynamical axion field in the material.

We now do an order-of-magnitude estimate of the size of this effect. The change in the polarization rotation depends on the size of the induced $g\delta\theta$ (recall $g = \alpha/\pi$ is a universal constant). Applying the equations of motion, we find that this will scale as $g\delta\theta \sim (g^2/\kappa)(E/\Omega)^2/c$, as $B \sim E/c$ in these units, and Ω is the dynamical axion resonance frequency which we take to be 10GHz. Up to numerical factors we take $\kappa = \nu(E_F) \sim k_F^2/v_F$ for a semimetal with Fermi velocity $v_F \sim 10^{-3}c$. k_F in turn is set by the carrier density, which we take to be $k_F \sim .1\text{\AA}^{-1}$. For a large but physically realizable electric field of order 1MV/cm this gives a response of $g\delta\theta \sim g^2 v_F / c E^2 / (\Omega k_F)^2 \sim 1.2$, which is a small but observable response.

Conclusion—Beginning with a Weyl semimetal with charge density wave order, we have shown how the separation of the Weyl nodes in tandem with the CDW-induced phase fluctuations can give rise to a dynamical axion field. To model the dynamical axion mode and determine a novel optical signature we solved the nonlinear partial differential equations describing its dynamics and established a two-step, pump-probe style protocol which excites this mode with a two-photon excitation scheme, and subsequently detects it with a third probe beam. The intensity of the axion excitation is stronger for parallel collinear beams relative to other beam configurations, as can be understood from Eq. (A11) and is shown in Fig. 2(c). Our key result is reflected probe beam's Kerr

angle is modulated such that it approximately tracks the axion field oscillation.

A motivation of this work is to provide theoretical predictions that can drive future experimental work, where potential material candidates could include axion insulators MnBi_2Te_4 [30] and $(\text{TaSe}_4)_2\text{I}$ [22, 31, 32]. This paper has demonstrated the potential for mutlidimensional [33–35] and multiphoton spectroscopy in the study of correlated topological materials and their dynamics [36]. The Quantum Chromodynamics axion, possibly within reach of experimental verification by current experiments, represents one of the most compelling pathways beyond the Standard Model, by providing at the same time an elegant solution to the strong CP problem and an excellent dark matter candidate [3, 37]. Meanwhile, condensed matter axions arising in novel, topological materials has lead to a more accessible playground for studying the exotic phenomena associated with these particles that may provide insight when mapped back to high energy physics and impact experimental prospects of an axion discovery via axion-mediated forces. Our work also has implications for condensed matter axion systems that are being used to detect their high energy counterparts in direct detection dark matter experiments [38, 39].

ACKNOWLEDGMENTS

The authors would like to acknowledge fruitful discussions with Aaron Chou, Fahad Mahmood, Soyeun Kim, Ankit Disa, and Yikun Wang. This work is entirely supported by the Quantum Science Center (QSC), a National Quantum Information Science Research Center of the U.S. Department of Energy (DOE). P.N. gratefully acknowledges support from the Gordon and Betty Moore Foundation grant number #8048 and from the John Simon Guggenheim Memorial Foundation (Guggenheim Fellowship).

Appendix A: Derivation of axion response function

Here we provide more detailed derivations of the results presented in the main work. We begin by outlining the steps to excite the axion mode via two externally applied light beams, and arrive at the axion response function. To start, we show how the gauge field and axion equations of motion may be derived from the full axion modified electromagnetic Lagrangian

$$\mathcal{L} = \frac{1}{2}(\epsilon \mathbf{E}^2 - \frac{1}{\mu} \mathbf{B}^2) + g\theta \mathbf{E} \cdot \mathbf{B} + \frac{\kappa}{2}[(\partial_t \delta\theta)^2 - v^2(\nabla \delta\theta)^2 - \Omega_0^2 \delta\theta^2] \quad (\text{A1})$$

by utilizing the Euler-Lagrange formalism. For \mathbf{A} this is

$$\frac{\partial}{\partial t} \left(\frac{\partial L}{\partial(\partial_t \mathbf{A})} \right) + \nabla \cdot \left(\frac{\partial L}{\partial(\nabla \mathbf{A})} \right) - \frac{\partial L}{\partial \mathbf{A}} = 0 \quad (\text{A2})$$

Varying with respect to \mathbf{A} yields its equation of motion

$$\partial_t^2 \mathbf{A} - \nabla \times \nabla \times \mathbf{A} = g(\partial_t \delta\theta \nabla \times \mathbf{A} - \nabla \delta\theta \times \partial_t \mathbf{A}) \quad (\text{A3})$$

Similarly for the axion field

$$\frac{\partial}{\partial t} \left(\frac{\partial L}{\partial(\partial_t \theta)} \right) + \nabla \cdot \left(\frac{\partial L}{\partial(\nabla \theta)} \right) - \frac{\partial L}{\partial \theta} = 0 \quad (\text{A4})$$

and the corresponding θ equation of motion

$$\kappa(\partial_t^2 + \gamma \partial_t - v^2 \nabla^2 + \Omega_0^2) \delta\theta = g[\partial_t \mathbf{A}(\nabla \times \mathbf{A})] \quad (\text{A5})$$

As stated in the main text, $v^2 \nabla^2 \theta$ may be dropped by observing $v \ll c$. The goal is to solve for the axion response to an externally applied electromagnetic field. This is first carried out by perturbatively expanding for θ and \mathbf{A} with small parameter ϵ

$$\mathbf{A}(\mathbf{x}, t) = \epsilon \mathbf{A}_1 + \epsilon^2 \mathbf{A}_2 + \epsilon^3 \mathbf{A}_3 + \dots \quad (\text{A6})$$

$$\theta(\mathbf{x}, t) = \epsilon \theta_1 + \epsilon^2 \theta_2 + \epsilon^3 \theta_3 + \dots \quad (\text{A7})$$

Performing this expansion and plugging into the gauge field and axion equations of motion, respectively, determines the axion field must be minimally excited by two gauge fields. With this in mind, we solve for $\delta\theta$ by Fourier transforming Eq. (A5). Note the vector potential Fourier transforms as $\mathbf{A}(x_i) = \int_q e^{iq_i \cdot x} \mathbf{A}(q_i)$; and we denote $\int_q = \int \frac{d^3 q}{(2\pi)^3} \int \frac{d\Omega}{2\pi}$, and $q \cdot x = \mathbf{q} \cdot \mathbf{x} - \Omega t$ in the exponential.

$$\begin{aligned} & \kappa \int d^4 x e^{-iq \cdot x} (\partial_t^2 + \gamma \partial_t + \Omega_0^2) \delta\theta(x) = \\ & \kappa(-\Omega^2 + i\Omega + \Omega_0^2) \int d^4 x e^{-iq \cdot x} \delta\theta(x) = \\ & \kappa(-\Omega^2 + i\Omega + \Omega_0^2) \delta\theta(q) \end{aligned} \quad (\text{A8})$$

Inverting the matrix $(-\Omega^2 + i\Omega + \Omega_0^2)\mathbb{I}$ to isolate $\delta\theta(q)$ on the left-hand side:

$$\begin{aligned} \delta\theta(q, \omega) &= [-\Omega^2 + i\Omega + \Omega_0^2]^{-1} \left(\frac{g}{\kappa} \right) \times \\ & \int d^4 x e^{-iq \cdot x} [\partial_t \mathbf{A}(x_1) \cdot \nabla \times \mathbf{A}(x_1)] \\ &= [-\Omega^2 + i\Omega + \Omega_0^2]^{-1} \left(\frac{g}{\kappa} \right) \times \\ & \int d^4 x e^{-iq \cdot x} [\partial_t \int e^{iq_1 \cdot x} \mathbf{A}_1(q_1) \cdot \nabla \times \int e^{iq_2 \cdot x} \mathbf{A}_1(q_2)] \\ &= [-\Omega^2 + i\Omega + \Omega_0^2]^{-1} \left(\frac{g}{\kappa} \right) \int_{q_1, q_2} \int_q d^4 x \times \\ & e^{-i(q \cdot x - q_1 \cdot x - q_2 \cdot x)} (-i\Omega_1 \mathbf{A}_1(q_1)) (i\mathbf{q}_2 \times \mathbf{A}_1(q_2)) \end{aligned} \quad (\text{A9})$$

Making use of the exponential representation as the Dirac delta function $\int d^4 x e^{-i(q \cdot x - q_1 \cdot x - q_2 \cdot x)} = \delta_{q_1 + q_2, q}$ simplifies this to

$$\begin{aligned} \theta_2(q) &= [-\Omega^2 + \Omega_0^2]^{-1} \left(\frac{g}{\kappa} \right) \times \\ & \int_{q_1, q_2} \delta_{q_1 + q_2, q} \Omega_1 \mathbf{A}_1(q_1) \cdot (\mathbf{q}_2 \times \mathbf{A}_1(q_2)). \end{aligned} \quad (\text{A10})$$

Recall the field is minimally composed of two beams whose frequencies must add up to axion resonance $\Omega = \omega_1 + \omega_2$ in order to excite the mode. Utilizing a plane-wave ansatz $\mathbf{A}(q) = \mathbf{A}_1\delta_{q,q_1} + \mathbf{A}_2\delta_{q,q_2}$, with four-momenta $q_i = (\omega_i, \mathbf{q}_i)$ for frequency ω_i and momentum \mathbf{q}_i ; the solution for the axion field is

$$\delta\theta(\omega_1, \omega_2, \mathbf{q}_1, \mathbf{q}_2) = \frac{(g/\kappa)(\omega_2\mathbf{q}_1 - \omega_1\mathbf{q}_2) \cdot (\hat{\mathbf{E}}_1 \times \hat{\mathbf{E}}_2)}{(\omega_1 + \omega_2)^2 + i(\omega_1 + \omega_2)\gamma - \Omega_0^2} A_1 A_2 \quad (\text{A11})$$

Appendix B: Axion modified electrodynamics

Next consider the interface of a dynamical axion insulator (DAI) and a vacuum. The side of the vacuum is governed by the sourceless Maxwell's equations; while the other side is the DAI governed by axion electrodynamics with modified constitutive equations

$$\mathbf{D} = \epsilon\mathbf{E} - g\theta\mathbf{B} \quad (\text{B1})$$

$$\mathbf{H} = \frac{1}{\mu}\mathbf{B} + g\theta\mathbf{E} \quad (\text{B2})$$

where $\epsilon = \epsilon(\mathbf{r}, t)$ is the complex dielectric tensor and $\mu = \mu(\mathbf{r}, t)$ is the magnetic permeability tensor which we set to 1 for simplicity, as is the case in nonmagnetic materials. In the medium, modified Ampere's law gives

$$\nabla \times \mathbf{H} = \mathbf{J} + \partial_t \mathbf{D} \rightarrow \quad (\text{B3})$$

$$\nabla \times \left(\frac{1}{\mu_0} \mathbf{B} + g\theta\mathbf{E} \right) = \mathbf{J} + \partial_t (\epsilon\mathbf{E} - g\theta\mathbf{B}) \quad (\text{B4})$$

where $\mathbf{J} = \sigma\mathbf{E}$ and we include in the conductivity σ the contribution from the Hall conductivity. Substituting back in for the vector potential gives and simplifying $\frac{1}{\mu}\nabla \times \nabla \times \mathbf{A} = \epsilon(\mathbf{r})\partial_t^2 \mathbf{A}$ and so far it is assumed θ does not spatially vary. As stated in the main text, we take the adiabatic approximation for now and let $\dot{\theta} = 0$. Later θ will be promoted to be time-dependent. Fourier-transforming equation this expression

$$\frac{1}{\mu} (i\mathbf{k} \times i\mathbf{k} \times \mathbf{A}) = \epsilon(\omega)\omega^2 \mathbf{A} \rightarrow \quad (\text{B5})$$

$$\frac{1}{\mu} (\mathbf{k} \cdot \mathbf{k} \mathbb{I} - \mathbf{k} \otimes \mathbf{k}) \mathbf{A} = \epsilon(\omega)\omega^2 \mathbf{A} \quad (\text{B6})$$

To simplify this slightly, let the incident and reflected light propagate in the \hat{z} -direction and let this be orthogonal to the interface whose surface lies in the xy -plane. Then due to boundary conditions the wave-vector of the transmitted light will also be along the \hat{z} -direction so that $\mathbf{k} = (0, 0, k_z)$. This simplifies the above matrix equation as

$$\begin{pmatrix} k_z\omega^2 & 0 \\ 0 & k_z\omega^2 \end{pmatrix} \begin{pmatrix} A_x \\ A_y \end{pmatrix} = \omega^2 \begin{pmatrix} \epsilon_{xx} & \epsilon_{xy} \\ \epsilon_{yx} & \epsilon_{yy} \end{pmatrix} \begin{pmatrix} A_x \\ A_y \end{pmatrix} \quad (\text{B7})$$

Let the permittivity tensor have the form for a gyroelectric medium at frequency ω

$$\epsilon(\omega) = \begin{pmatrix} \epsilon_1(\omega) & i\epsilon_2(\omega) & 0 \\ -i\epsilon_2(\omega) & \epsilon_1(\omega) & 0 \\ 0 & 0 & \epsilon_3(\omega) \end{pmatrix} \quad (\text{B8})$$

Where we can ignore the z-component $\epsilon_3(\omega)$ which is zero for a plane-wave propagating in the z-direction. Solving the matrix equation B7 the eigenvalues correspond to $\mathbf{k}^\pm = \omega\sqrt{\epsilon_1 \pm \epsilon_2}\hat{e}^\pm$ and the eigenvectors form a chiral basis $\mathbf{A}_j^\pm = A_j^\pm \frac{1}{\sqrt{2}} \begin{pmatrix} 1 \\ \pm i \end{pmatrix}$. The incident field may be rewritten in the new chiral basis

$$\mathbf{A}_i = \mathbf{A}_i^+ \hat{e}_+ + \mathbf{A}_i^- \hat{e}_- \quad (\text{B9})$$

similarly for reflected and transmitted light.

Now let's promote θ to be time-dependent. Solving the nonlinear partial differential equation given in Eq. (A5) for time varying electromagnetic fields yields a dynamical contribution $\delta\theta$ to the axion field. This requires an expression for the pump beam $p(t) \propto \mathbf{E} \cdot \mathbf{B}$ to drive the axion mode, taken as a Gaussian wavepacket $p(t) = e^{(t/\sigma)^2} \cos(\Omega_0 t)$, where σ tunes the spread of the Gaussian, and Ω_0 denotes the axion resonant frequency. Thus the axion term will be a dynamical fluctuating field, which we later use to demonstrate how such a dynamical axion field generates a time-dependent modulation of the Kerr rotation.

Appendix C: Boundary conditions and Kerr rotation angle

The boundary conditions for electric and magnetic fields at an interface with no surface charge or current are

$$\mathbf{E}_i + \mathbf{E}_r = \mathbf{E}_t \quad (\text{C1})$$

$$\mathbf{B}_i + \mathbf{B}_r = \mathbf{B}_t + g\theta\mathbf{E}_t \quad (\text{C2})$$

where the left-hand-side of the equals sign is the vacuum and the right-hand-side is the DAI. In the vacuum $\mathbf{k} = \omega\hat{z}$ and in the DAI $\mathbf{k} = k^\pm\hat{z}$ as above. The boundary condition for electric field gives the simple condition $\mathbf{A}_i + \mathbf{A}_r = \mathbf{A}_t$. While the boundary condition for magnetic field must be considered further. Substituting back in for the vector potential

$$\sum_{\alpha=\pm} -i\mathbf{k}_i \times \mathbf{A}_i^\alpha + i\mathbf{k}_r \times \mathbf{A}_r^\alpha = -i\mathbf{k}_t^\alpha \times \mathbf{A}_t^\alpha - ig\theta\omega\mathbf{A}_t^\alpha \rightarrow \quad (\text{C3})$$

$$\sum_{\alpha} -i\omega\hat{z} \times \mathbf{A}_i^\alpha + i\omega\hat{z} \times \mathbf{A}_r^\alpha = -ik^\alpha\hat{z} \times \mathbf{A}_t^\alpha - ig\theta\omega\mathbf{A}_t^\alpha \quad (\text{C4})$$

here let $\alpha = \pm$. Plugging in for the vector potentials in the chiral basis and noting $\hat{z} \times \hat{e}_{\pm} = \pm i\hat{e}_{\pm}$

$$\hat{e}_+ : \omega I^+ - \omega R^+ = (k^+ - ig\theta\omega)T^+ \quad (\text{C5})$$

$$\hat{e}_- : \omega I^- - \omega R^- = (k^- + ig\theta\omega)T^- \quad (\text{C6})$$

Using $I^+ + R^+ = T^+$ and $I^- + R^- = T^-$ and solving for the R^{\pm} gives:

$$R^+ = \frac{\omega - (k^+ - ig\theta\omega)}{\omega + (k^+ - ig\theta\omega)} I^+ \quad (\text{C7})$$

Similarly for R^- :

$$R^- = \frac{-\omega + (k^- + ig\theta\omega)}{-\omega - (k^- + ig\theta\omega)} I^- \quad (\text{C8})$$

recall $k^{\pm} = \omega\sqrt{\epsilon_1 \pm \epsilon_2}$. The same can be done for the transmission coefficients:

$$T^+ = \frac{2\omega}{\omega + (k^+ - ig\theta\omega)} I^+ \quad (\text{C9})$$

$$T^- = \frac{2\omega}{\omega + (k^- + ig\theta\omega)} I^- \quad (\text{C10})$$

Finally, the Kerr rotation angle is related to the argument of the complex reflection amplitudes $R^{\pm} = |R^{\pm}|e^{i\Delta^{\pm}}$ as

$$\Theta_K = -\frac{1}{2}(\Delta^+ - \Delta^-) \quad (\text{C11})$$

-
- [1] R. D. Peccei and H. R. Quinn, CP conservation in the presence of pseudoparticles, *Phys. Rev. Lett.* **38**, 1440 (1977).
- [2] R. D. Peccei and H. R. Quinn, Constraints imposed by CP conservation in the presence of pseudoparticles, *Phys. Rev. D* **16**, 1791 (1977).
- [3] F. Chadha-Day, J. Ellis, and D. J. E. Marsh, Axion dark matter: What is it and why now?, *Science Advances* **8**, eabj3618 (2022), <https://www.science.org/doi/pdf/10.1126/sciadv.abj3618>.
- [4] D. Nenno, C. Garcia, J. Gooth, C. Felser, and P. Narang, Axion physics in condensed-matter systems, *Nat. Rev. Phys.* **2**, 682 (2020).
- [5] R. Li, J. Wang, X.-L. Qi, and S.-C. Zhang, Dynamical axion field in topological magnetic insulators, *Nature Physics* **6**, 284 (2010), 0908.1537.
- [6] Z. Wang and S.-C. Zhang, Chiral anomaly, charge density waves, and axion strings from Weyl semimetals, *Physical Review B* **87**, 161107 (2013), 1207.5234.
- [7] B. Roy and J. D. Sau, Magnetic catalysis and axionic charge density wave in Weyl semimetals, *Physical Review B* **92**, 125141 (2015), 1406.4501.
- [8] X. Wan, A. M. Turner, A. Vishwanath, and S. Y. Savrasov, Topological semimetal and Fermi-arc surface states in the electronic structure of pyrochlore iridates, *Physical Review B* **83**, 205101 (2011), 1007.0016.
- [9] S. D. Pace, C. Castelnovo, and C. R. Laumann, Dynamical Axions in $\mathbb{S}U(1)$ Quantum Spin Liquids, *arXiv* (2021), 2109.06890.
- [10] A. Sekine and K. Nomura, Axion electrodynamics in topological materials, *Journal of Applied Physics* **129**, 141101 (2020).
- [11] A. A. Zyuzin, S. Wu, and A. A. Burkov, Weyl semimetal with broken time reversal and inversion symmetries, *Physical Review B* **85**, 165110 (2012), 1201.3624.
- [12] A. M. Essin, J. E. Moore, and D. Vanderbilt, Magnetoelectric Polarizability and Axion Electrodynamics in Crystalline Insulators, *Physical Review Letters* **102**, 146805 (2009), 0810.2998.
- [13] A. A. Zyuzin and A. A. Burkov, Topological response in weyl semimetals and the chiral anomaly, *Phys. Rev. B* **86**, 115133 (2012).
- [14] W. Shi, B. J. Wieder, H. L. Meyerheim, Y. Sun, Y. Zhang, Y. Li, L. Shen, Y. Qi, L. Yang, J. Jena, P. Werner, K. Koepf, S. Parkin, Y. Chen, C. Felser, B. A. Bernevig, and Z. Wang, (A charge-density-wave topological semimetal, *Nat. Phys.* **17**, 381 (2021).
- [15] N. S. Srivatsa and R. Ganesh, Excitonic collective modes in Weyl semimetals, *Physical Review B* **98**, 165133 (2018), 1808.05233.
- [16] B. J. Wieder, K.-S. Lin, and B. Bradlyn, Axionic band topology in inversion-symmetric Weyl-charge-density waves, *Physical Review Research* **2**, 042010 (2020), 2004.11401.
- [17] D. Sehayek, M. Thakurathi, and A. A. Burkov, Charge density waves in Weyl semimetals, *Physical Review B* **102**, 115159 (2020), 2007.07256.
- [18] R. C. McKay and B. Bradlyn, Optical response from charge-density waves in Weyl semimetals, *Physical Review B* **104**, 155120 (2021), 2106.09577.
- [19] J. Curtis, I. Petrides, and P. Narang, Finite-Momentum Instability of Dynamical Axion Insulator, *Phys. Rev. B* **107**, 205118 (2023).
- [20] B. Zhao, C. Guo, C. A. C. Garcia, P. Narang, and S. Fan, Axion-Field-Enabled Nonreciprocal Thermal Radiation in Weyl Semimetals, *Nano Letters* **20**, 1923 (2020), 1911.08035.
- [21] C. R. Otey, W. T. Lau, S. Fan, *et al.*, Thermal rectification through vacuum, *Physical review letters* **104**, 154301 (2010).
- [22] J. Gooth, B. Bradlyn, S. Honnali, C. Schindler, N. Kumar, J. Noky, Y. Qi, C. Shekhar, Y. Sun, Z. Wang, B. A. Bernevig, and C. Felser, Axionic charge-density wave in the weyl semimetal (TaSe4)2i, *Nature* **575**, 315 (2019).
- [23] J. Yu, B. J. Wieder, and C.-X. Liu, Dynamical piezomagnetic effect in time-reversal-invariant Weyl semimetals with axionic charge density waves, *Physical Review B* **104**, 174406 (2021), 2008.10620.

- [24] T. Zhu, H. Wang, H. Zhang, and D. Xing, Axionic surface wave in dynamical axion insulators, arXiv (2022), 2204.06332.
- [25] L. Wu, M. Salehi, N. Koirala, J. Moon, S. Oh, and N. P. Armitage, Quantized Faraday and Kerr rotation and axion electrodynamics of a 3D topological insulator, *Science* **354**, 1124 (2016).
- [26] J. Ahn, S.-Y. Xu, and A. Vishwanath, Theory of optical axion electrodynamics and application to the Kerr effect in topological antiferromagnets, *Nat. Comm.* **13**, 7614 (2022).
- [27] B. Yan and C. Felser, Topological materials: Weyl semimetals, *Annual Review of Condensed Matter Physics* **8**, 337 (2017), <https://doi.org/10.1146/annurev-conmatphys-031016-025458>.
- [28] A. Burkov, Weyl metals, *Annual Review of Condensed Matter Physics* **9**, 359 (2018), <https://doi.org/10.1146/annurev-conmatphys-033117-054129>.
- [29] In some cases it is also possible to have a separation of the Weyl nodes in energy of Q_0 , leading to an additional contribution of $Q_0 t$ in the static axion. This leads to additional topological responses but we will not consider this case here.
- [30] D. Zhang, M. Shi, T. Zhu, D. Xing, H. Zhang, and J. Wang, Topological axion states in the magnetic insulator mnbi_2te_4 with the quantized magnetoelectric effect, *Phys. Rev. Lett.* **122**, 206401 (2019).
- [31] S. Kim, R. McKay, *et al.*, Kramers-Weyl fermions in the chiral charge density wave material $(\text{TaSe}_4)_2\text{I}$ (2021), arXiv:2108.10874.
- [32] Q. Nguyen, R. Duncan, *et al.*, Ultrafast x-ray scattering reveals composite amplitude collective mode in the Weyl charge density wave material $(\text{TaSe}_4)_2\text{I}$ (2022), arXiv:2210.17483.
- [33] Z. Zhang, F. Gao, *et al.*, Nonlinear coupled magnonics: Terahertz field-driven magnon upconversion (2022), arXiv:2207.07103.
- [34] Z. Zhang, F. Gao, *et al.*, Three-wave mixing of anharmonically coupled magnons (2023), arXiv:2301.12555.
- [35] M. Mootz, L. Luo, J. Wang, and I. Perakis, Visualization and quantum control of light-accelerated condensates by terahertz multi-dimensional coherent spectroscopy, *Comm. Phys.* **5**, 47 (2022).
- [36] M. Rodriguez-Vega, Z.-X. Lin, A. Leonardo, A. Ernst, M. Vergniory, and G. Fiete, Light-Driven Topological and Magnetic Phase Transitions in Thin Layer Antiferromagnets, *J. Phys. Chem. Lett.* **14**, 4152 (2022).
- [37] R. D. Peccei and H. R. Quinn, CP conservation in the presence of pseudoparticles, *Phys. Rev. Lett.* **38**, 1440 (1977).
- [38] J. Schütte-Engel, D. J. Marsh, A. J. Millar, A. Sekine, F. Chadha-Day, S. Hoof, M. N. Ali, K. C. Fong, E. Hardy, and L. Šmejkal, Axion quasiparticles for axion dark matter detection, *Journal of Cosmology and Astroparticle Physics* **2021** (08), 066.
- [39] S. Chigusa, T. Moroi, and K. Nakayama, Axion hidden-photon dark matter conversion into condensed matter axion, *Journal of High Energy Physics* **2021**, 10.1007/jhep08(2021)074 (2021).